PROMPT FISSION NEUTRON MULTIPLICITY INVESTIGATION

Sh. Zeynalov[a], O. Zeynalova[a], F.-J. Hambsch[b], S. Oberstedt[b]

[a)]JINR-Joint Institute for Nuclear Research, Dubna Moscow region, Russia
[b)]EC JRC Institute for Reference Materials and Measurements, Retieseweg 111, 2440 Geel, Belgium

Abstract

The present work focuses on investigating the non-linear dependence of the average prompt fission neutron (PFN) multiplicity as a function of the total kinetic energy (TKE) of the fission fragments (FF) by using modern digital signal processing (DSP). A twin Frisch-grid ionization chamber (TGIC) was used for FF mass and kinetic energy spectroscopy. A fast NE213 equivalent liquid scintillation neutron detector (ND) was used for the PFN time-of-flight measurement. About 10^7 fission events coincident with PFN detection were acquired in the experiment. Correlated FF kinetic energies, the angle between the fission axis and the PFN and the PFN velocity were measured with an eight channel waveform digitizers (WFD) system, having 100 MHz sampling frequency and 12 bit pulse height resolution. Analysis of the acquired data revealed effects, causing distortion of the measured angular distribution of PFN and the dependence of their average number on TKE of the FF. Special modification of the experiment and respective modifications in the data analysis procedure has resulted in a reasonable agreement between experimental results and theoretical calculations. For the first time a linear dependence of the PFN multiplicity on TKE in the range of (140 – 220) MeV is demonstrated. A new measurement set-up in experiments with actinide targets like ^{235}U, ^{239}Pu, etc. is proposed.

Introduction

The purpose of the present experiment was to study the details of prompt fission neutron (PFN) emission in spontaneous fission of ^{252}Cf. The experimental method was adopted from Ref. [1] replacing the analogue electronics with modern digital pulse processing hardware/software. The measurement of correlated fission fragment (FF) kinetic energies by a double ionization chamber allowed the determination of FF masses, velocities and angles between FF and the PFN, coinciding with FF detection. In the current experiment the reconstruction of PFN emission kinematics was done carefully taking into account corrections due to various effects distorting the results of the measurement. The advantage provided by the digital pulse processing allowed to resolve some longstanding contradictions between theoretical calculations and experimental results.

Experimental setup

The anode current caused by a fission fragment (FF) in the TGIC was amplified by a charge-sensitive pre-amplifier and sampled with a 12 bit, 100 Ms/sec waveform digitizer

(WFD). The step-like long anode signals were software-wise transformed into short current pulses, which allowed effective pulse pile-up elimination. The anode current pulses were used to determine the fission fragment angle with respect to the cathode-plane normal. Prompt fission neutron (PFN) time-of-flight (TOF) spectroscopy was performed after passing the neutron detector (ND) pulse, digitized with a 12 bit WFD and a rate of 100 Ms/sec, through a 12^{th} order digital low pass filter. The ND pulse shape discrimination was implemented using raw-signal waveforms. The measurement of the FF characteristics, both in coincidence and non-coincidence with the PFN, was done without re-adjusting the apparatus. A Cf-sample with an activity of about 500 fission/sec, deposited on a 100 μg/cm^2 thick Ni foil was mounted on the common cathode of the twin Frisch-grid ionization chamber (TGIC), which operated with P-10 under atmospheric pressure as working gas at a constant flow between 50 and 100 ml/min. About 1.2×10^7 coincidences between FF and PFN signals were acquired in the measurement, which is comparable to the statistics reported in Ref. [1].

Experimental method and results

The detailed information on PFN emission in fission is available from the measured dependence of the average PFN multiplicity on the mass number A and the TKE of the fissile nucleus - $\bar{\nu}(A,TKE)$. Averaged characteristics on $\bar{\nu}(A)$ or $\bar{\nu}(TKE)$ by integrating over respective variable are obtained, if the FF mass yield matrix - *Y(A,TKE)* is known, for example:

$$\bar{\nu}(A) = \frac{\int_0^\infty \bar{\nu}(A,TKE)Y(A,TKE)dTKE}{\int_0^\infty Y(A,TKE)dTKE}, \qquad (1).$$

$$\bar{\nu} = \int_0^\infty \bar{\nu}(A,TKE)Y(A,TKE)dTKEdA, \quad 200 = \int_0^\infty Y(A,TKE)dTKEdA$$

Similar relations can be written for averaging over A:

$$\bar{\nu}(TKE) = \frac{\int_0^\infty \bar{\nu}(A,TKE)Y(A,TKE)dA}{\int_0^\infty Y(A,TKE)dA}, \qquad (2).$$

$$\bar{\nu} = \int_0^\infty \bar{\nu}(A,TKE)Y(A,TKE)dTKEdA, \quad 200 = \int_0^\infty Y(A,TKE)dTKEdA$$

$\nu(A),\nu(TKE)$ can be easily determined if the distributions of $\nu(A,TKE)$ and $Y(A,TKE)$ are known. To do so for each fission event the FF and PFN kinetic energies, FF masses along with the angle between PFN and FF motion should be determined. All this information can then be used to reconstruct the PFN emission kinematics both in the laboratory (LF) and in the centre of mass (CMF) frames. Possible explanation of the discrepancies in the results of experiments from refs. [2-6] might stem from significant systematic errors in the kinematics parameters of the FF. In the measurement method of FF mass and kinematics parameters we carefully verified the data analysis procedure taking into account the new possibilities provided by the digital signal processing. The measurements were carried out using the experimental setup presented in Fig. 1.

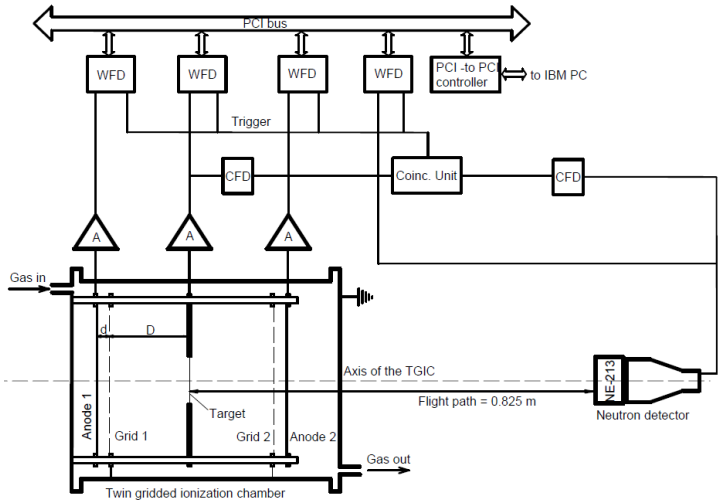

FIGURE 1. Experimental setup

The two angular distributions of correlated FF, measured in the LF are presented in fig. 2a. The angle between the FF and the PFN was measured using half of the TGIC from the layer side in one of the measurements and from the target backing side in the other measurement. Comparison of the curves in fig. 2a (obtained after energy loss and grid inefficiency corrections were applied) demonstrates a significant difference, increasing for the angles close to 90º. Apparently, the observed anisotropy distortion in the LF is due to energy losses in the target backing. After transformation to the CMF during data analysis this effect might cause systematic errors, distorting the reaction kinematics.

The background created by the second FF to the PFN emission of the first one was investigated in Ref. [1] and was modified in our approach. According to the reaction kinematics depicted in fig. 2b, the kinetic energy of the second FF in the CMF, must be much higher than the kinetic energy of the first FF. Bearing in mind the exponential drop of the PFN energy spectrum in the CMF, the contribution to the PFN from both FFs could be evaluated using the probabilities defined as:

$$W_1 = \frac{1}{N}\exp(\frac{-E_1}{N}),\ W_2 = \frac{1}{N}\exp(\frac{-E_2}{N}),\ W_1 + W_2 = 1 \qquad (3),$$

where W_1/W_2 - are probabilities of PFN emission and E_1/E_2 - are the kinetic energies of first and second FF respectively, the parameter N is a normalization factor. A comparison of the mass distributions plotted using measured data and probabilities, defined by eq. (3) are presented in fig. 3a. Results are in agreement with ref. [1], where the background from the complementary fragments was found to be small. The transformation of the measured angular distribution of the FF in the CMF, where the cos(Θ) was measured in the target layer half of the TGIC is plotted in fig. 3b, proving that more than 99% of the PFN are emitted from fully accelerated FFs. The transformation from LF to CMF was done using the following formula:

$$\Omega_{CM}(v_{CM},\Theta_{CM})dv_{CM}\,d\cos(\Theta_{CM}) = \frac{v_{CM}}{v_{lab}}\Omega_{lab}(\mathrm{v}_{\mathrm{lab}}(v_{CM},\Theta_{CM}),\Theta_{lab}(v_{CM},\Theta_{CM})) \qquad (4)$$

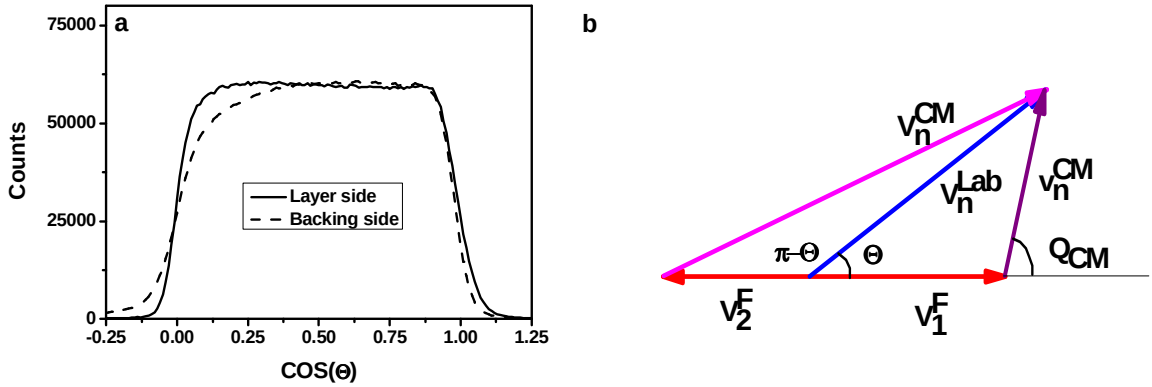

FIGURE 2. a.)FF angular distribution measured for the ^{252}Cf(sf) reaction within half of the TGIC from the layer side (solid line) and from the backing side (dashed line) in LF. b.) ^{252}Cf(sf) reaction kinematics.

The average PFN multiplicity as a function of FF mass number, evaluated from the experiment based on the described method above is presented in fig. 4a in comparison with literature data [1, 7]. The saw-tooth like shape of the PFN distribution is explained in a model proposed by Brosa et al. [8] making two main assumptions: multi-modal fission and random neck rupture (MM-RNR). The model provides the link between the experimentally measured configuration, asymmetry and neck shape of the fissile nucleus. In addition, the distribution $\bar{\nu}(A,TKE)$ contains information on neck elasticity as well as on the partition of the excitation energy between both FFs. The dependence of the PFN multiplicity as a function of TKE is presented in fig. 4b in comparison with data from Ref. [1] and theoretical calculations from Ref. [9].

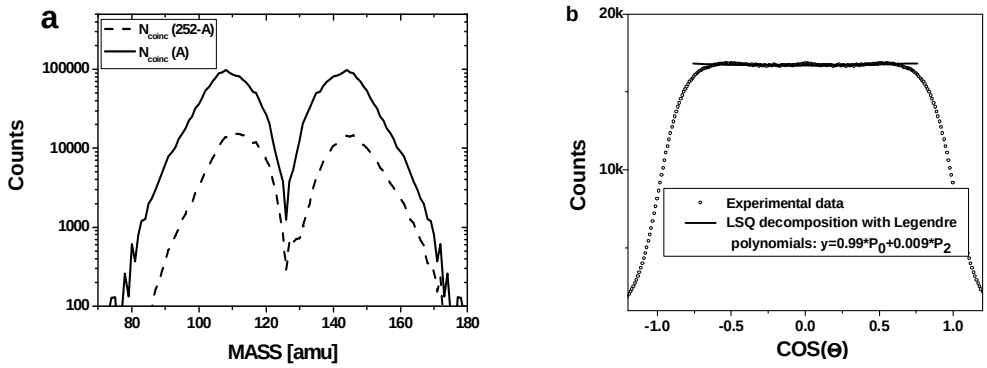

FIGURE 3. a) Relative contribution to the PFN of investigated FF from the complementary FF as a function of the mass split. **b)** PFN angular distribution in the CMF after correction for background neutrons from the correlated FF along with a fit with Legendre polynomials

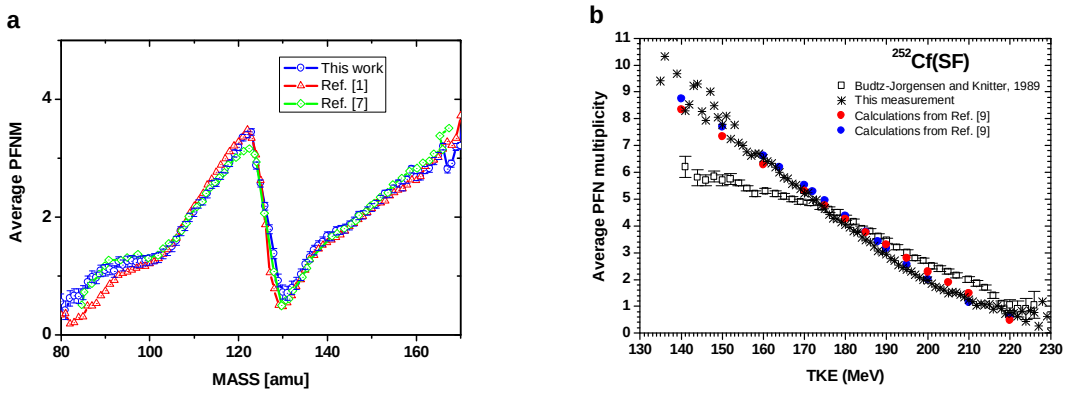

FIGURE 4. a) Dependence of average PFN multiplicity on FF mass in comparison with literature [1, 7]. b) Dependence of average PFN multiplicity on TKE in comparison with literature and theoretical calculations [9].

Outlook and conclusion

A modification of the TGIC made recently provides the possibility of the measurement of the FF axis orientation in 3D. The anodes of the TGIC are made position sensitive thanks to splitting them into two electrically isolated parts as shown in the left part of fig. 5 (backgammon method). The motion of the electrons in the grid-anode space induces an electric current shared by the two parts of the anode. The difference between instant currents is zero when the electrons are close to the line dividing the anode into two symmetric parts (ML-middle line). Deviation from this line to any direction perpendicular to the ML increases the current in the corresponding half of the electrode. This fact was, provides position sensitivity along a chosen direction. When anode of one half of TGIC is oriented along the X axis of the coordinate frame in the right side of fig. 5 and anode of the other side is oriented along the Y axis, the fission axis orientation in space can

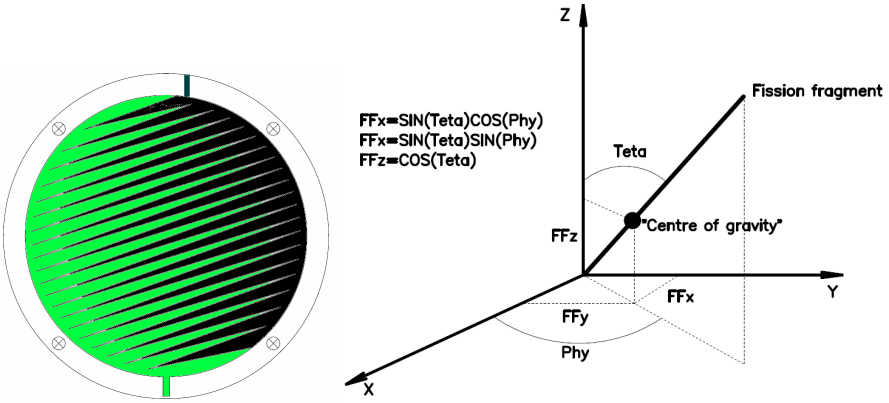

FIGURE 5. The anode of the position sensitive TGIC (left). Illustration of fission axis orientation evaluation in the coordinate frame with the z-axis directed along the TGIC axis (right).

be measured. Let the Z axis in fig. 5 be stretched along the TGIC axis, then the ionization chamber part of the experimental setup was modified as shown in fig. 6 leaving ND part unchanged. The charge sensitive preamplifiers in each anode circuit were replaced by two wideband current preamplifiers. Considering drift of electrons created during FF deceleration

inside the TGIC, the electric pulses at the preamplifier output can be used to evaluate the fission axis orientation in the coordinate frame of fig. 5 using the following approach. To measure the cosine of the angle Θ between the FF and the TGIC's axis the drift time method, utilizing the drift time dependence on Θ of electrons released by the FF, was implemented:

$$T[L] = \frac{\sum_{k=Tg}^{Tg+L} k * (I_1[k] + I_2[k])}{\sum_{k=Tg}^{Tg+L} (I_1[k] + I_2[k])} - T_g$$,where Tg is the trigger signal leading edge position, $I_1[k]$ and $I_2[k]$ are the sampled current pulses from the respective half of the anode. The trigger signal was obtained from the common cathode pulse and referred to as the time instant of the fission event. The dependence of cos(Θ) on the drift time can be found using the following formulae:

$T_{90} = \frac{D + 0.5 * d}{W}$, $T_{90} - T(E) = (T_{90} - T_0(\mathrm{E})) * \cos(\Theta)$, $P^C = \frac{P^O * T_{90}}{T_{90} + \sigma * T}$, where D and d are the cathode-grid and grid-anode distances, respectively, W is the free electron drift velocity, T_0, T_{90} are the drift times for FF having Θ equal to 0^o and 90^o, respectively, σ is the grid inefficiency, P^C, P^O are the grid inefficiency corrected and uncorrected total charges collected on the anodes and T is the drift time for the considered FF. The X_C coordinate of the FF

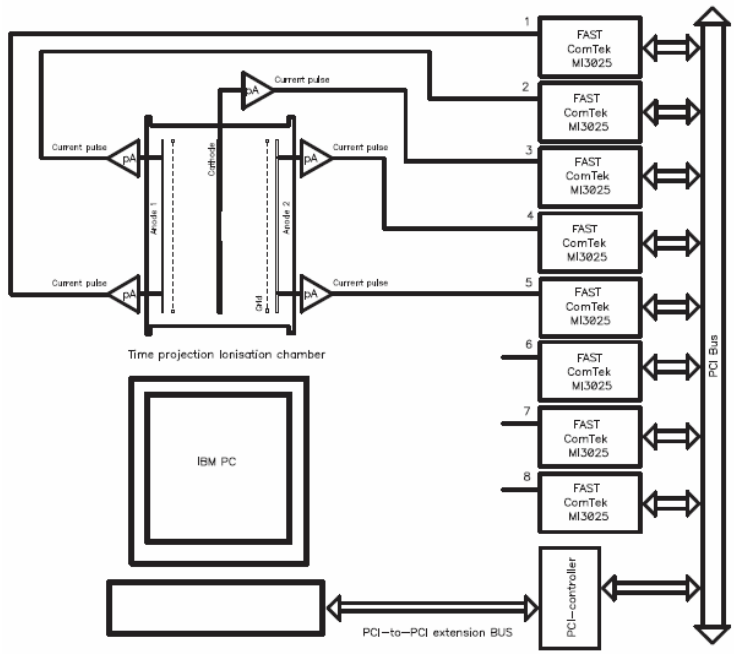

FIGURE 6. Modified experimental setup of the time position sensitive TGIC.

"centre of gravity" was found using the following equation $X_C = \frac{\sum_{k=Tg}^{Tg+L} k * (I_1[k] - I_2[k])}{\sum_{k=Tg}^{Tg+L} (I_1[k] + I_2[k])}$. In a similar way the Y_C coordinate of the correlated FF, detected in the other half of the TGIC,

was found. The angles between the fission axis and the coordinate axis were then found using the following equations:

$$X_C = R1 * SIN(\Theta) * COS(\Phi)$$
$$Y_C = R2 * SIN(\Theta) * SIN(\Phi) \qquad (5),$$

where R1, R2 are the average range of the FF, having known kinetic energies E1, E2, respectively. The ranges were supposed to be proportional to the maximum drift time known for each half of the chamber from a cos(Θ) calibration procedure similar to one used in ref. [1]. Finally the three cosines between the FF axis and the coordinate axis in fig. 5 were found:

$$COS(X) = SIN(\Theta) * COS(\Phi) = \frac{X_C}{R1},\ COS(Y) = SIN(\Theta) * SIN(\Phi) = \frac{Y_C}{R2},\ COS(Z) = COS(\Theta) \quad (6)$$

The modified experimental setup was used in a measurement of the spontaneous fission of ^{252}Cf to prove the above claimed properties of the TGIC. The angular distribution of FF measured for fixed intervals in COS(Θ) are plotted in fig. 7, demonstrating the angular sensitivity of the method. A preliminary evaluation of precision of the method gives about 0.1 as the averaged between the three cosine values. A more detailed evaluation is underway and should be done in the near future, but, nevertheless, the preliminary result is already quite promising. The position sensitive TGIC developed in this work opens a new perspective for future PFN investigation, especially for actinide targets like ^{235}U and ^{239}Pu.

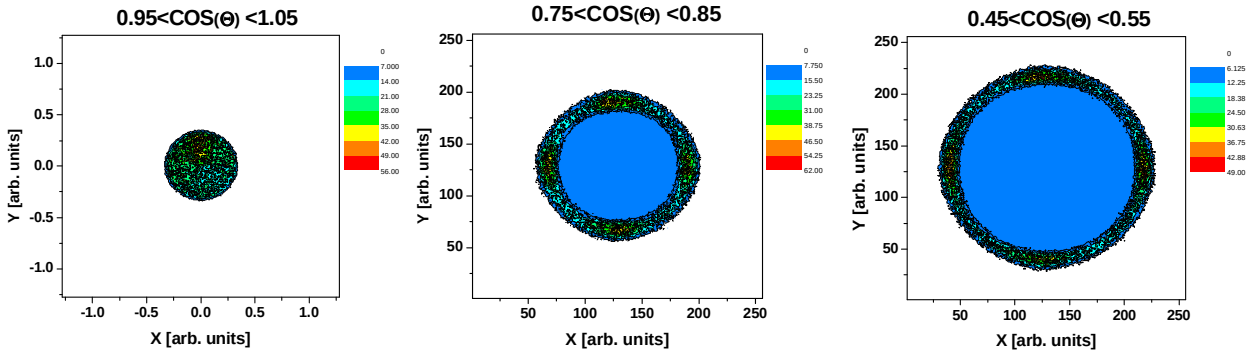

FIGURE 7. FF angular distributions measured for different fixed intervals in COS(Z).

Apparently targets from these nuclei cannot be made of negligible thickness, like for ^{252}Cf. Still the PFN investigation should be done in the full solid angle. Hence, positioning of an ND along the TGICs axis to simplify the measuring procedure does not work anymore. Here, our position-sensitive TGIC will allow to place additional ND off-axis, increasing considerably the experimental efficiency.

References

1. C. Budtz-Jorgensen and H.-H. Knitter, Nucl. Phys. A490 (1988) 307.
2. H.R. Bowman, S. G. Thompson, J. C. D. Milton, W. J. Swiatecki, Phys. Rev. 129 (1963), 2133.
3. K. Skarsvag, I. Singstad, Nucl. Phys. 62 (1965), 103.

4. A.S. Vorobyev, O.A. Sherbakov, Yu.S. Pleva, A.M. Gagarski, G.V.Valski, G.A.Petrov, V.I.Petrova, T.A. Zavarukhina, Nucl. Instr. Meth. A598 (2009), 795.
5. S.S. Kapoor, R. Ramanna, P.N. Rama Rao, Phys. Rev.131 (1963), 283.
6. M.S. Samant, R.P. Anand, R.K. Choudhury M. S. Samant, S. S. Kapoor, and D. M. Nadkarni, Phys. Rev. C51 (1995), 3127.
7. H. Nifenecker, C. Signarbieux, R. Babinet, J. Poitou, Symposium on Physics and Chemistry of Fission, 13-17 August, 1973, Rochester, N.Y., USA - Vienna: IAEA, 1974, Vol. 2 P. 117-178.
8. U. Brosa, S. Grossmann, A. Mũller, Phys. Report 197 (1990), 167.
9. A. Tudora, Ann. Nucl. Energy 35 (2008), 1.